Microstructure and optical properties of nitrogen-doped ZnO film*

Zhao Xian-Wei(赵显伟), Gao Xiao-Yong(郜小勇)†, Chen Xian-Mei(陈先梅), Chen Chao(陈 超), and Zhao Meng-Ke(赵孟珂)

Key Laboratory of Material Physics (Ministry of Education), School of Physics and Engineering, Zhengzhou University, Zhengzhou 450052, *China*

(Received 5 May 2012; revised manuscript received 17 July 2012)

The nitrogen doping of ZnO film deposited by the magnetron sputtering method is subsequently realized by the hydrothermal synthesis method. The nitrogen-doped ZnO film is preferably (002) oriented. With the increase of hexamethylenetetramine (HMT) solution concentration, the average grain size of the film along the ⟨002⟩ direction almost immediately decreases and then monotonously increases, conversely, the lattice strain first increases and then decreases. The structural evolution of the film surface from compact and even to sparse and rough is attributed to the enhanced nitrogen doping content in the hydrothermal process. The transmission and photoluminescence properties of the film are closely related to grain size, lattice strain, and nitrogen-related defect arising from the enhanced nitrogen doping content with HMT concentration increasing.

Keywords: nitrogen-doped ZnO film, hydrothermal method, optical properties

PACS: 42.30.Va, 42.70.Ce, 42.79.–e **DOI:** 10.1088/1674-1056/22/2/024202

1. Introduction

ZnO has a wide band gap of 3.37 eV at room temperature and a high exciton binding energy of 60 meV. Hence, it can be used in different functional devices such as light emitting diodes,[1–5] solar cells,[6] gas-sensitive sensors,[7,8] and photocatalysts.[9] In a solar cell, ZnO film can act as a transparent electrode and window layer that can enable most light beyond 370 nm to pass through and stimulate the pn junction to produce electrons and current. The high exciton binding energy of ZnO is very promising for the realization of devices such as ultraviolet (UV) light-emitting diodes and UV lasers beyond room temperature. Although ZnO films fabricated by different deposition methods have been intensively studied, attempts to improve device performance to meet application demands remain ongoing.

Considering native defects such as zinc interstitials and oxygen vacancies, intrinsic ZnO shows weak n-type conductivity. Many techniques such as magnetron sputtering,[2,8,10–12] pulsed laser deposition,[3] plasma-assisted molecular beam epitaxy technique,[1] sol–gel,[13,14] and electron beam evaporation method[15] have been adopted to fabricate (002) oriented ZnO on different substrates. Hydrothermal synthesis[6,7,16] is usually used to fabricate ZnO nanowires, nanorods, film, and powder. However, it is difficult to produce ZnO film with uniform texture and smooth surface by hydrothermal synthesis. In the present paper, ZnO films are first fabricated on a glass substrate and this is followed by nitrogen doping in a hexamethylenetetramine (HMT) solution by the hydrothermal method to obtain the improved nitrogen-doped ZnO films. The effects of the HMT solution concentration on the microstructure, transmission, and photoluminescence (PL) of the films are examined.

2. Experimental procedure

First, 266-nm-thick ZnO films were fabricated on glass substrates by direct-current magnetron sputtering. To avoid unfavorable effects on film quality, the quartz glass substrates were sequentially rinsed with acetone, propyl alcohol, dehydrated alcohol, and deionized water in an ultrasonic bath for 15 min. The detailed preparation parameters of the ZnO film are listed as follows: substrate temperature of 200 °C, working pressure of 0.7 Pa, oxygen-to-argon mass flow ratio of 3.0:18.0, and sputtering power of 120 W to 130 W.

The ZnO-covered glass substrates were then placed in HMT solution and allowed to react for 24 h at 95 °C in a Teflon-lined stainless reactor to realize nitrogen doping. After naturally cooling the final reaction solution to room temperature, the products were washed with deionized water and dried for 24 h at 80 °C in a ventilation oven. In the hydrothermal process, HMT only acts as the dopant source. HMT can be hydrolyzed at high temperatures via the following reactions:[1]

$$(CH_2)_6N_4 + 10H_2O \leftrightarrow 6HCHO + 4NH_3 \cdot H_2O, \quad (1)$$

$$NH_3 + H_2O \leftrightarrow NH_4^+ + OH^-, \quad (2)$$

$$NH_3 \rightarrow (NH)_2^- + 2H^+, \quad (3)$$

$(NH)_2^-$ can break down zinc–oxygen bonds and form zinc–nitrogen bonds, nitrogen–oxygen bonds, and other defects.

*Project supported by the National Natural Science Foundation of China (Grant No. 60807001), the Foundation of Henan Educational Committee, China (Grant No. 2010A140017), the the Foundation of Young Key Teachers from University of Henan Province, China (Grant No. 2011GGJS-008), and the Graduate Innovation of Zhengzhou University, China (Grant No. 11L10102).

†Corresponding author. E-mail: xygao@zzu.edu.cn

© 2013 Chinese Physical Society and IOP Publishing Ltd

The surface morphology and crystalline structure of the nitrogen-doped film were characterized by a field-emission scanning electron microscope (JSM-6700) and X-ray diffractometer (Philips PANA-lytical X'pert) with CuKα (λ = 0.1540598 nm) radiation source. The transmission and PL spectra were obtained using a spectrophotometer (Shimadzu UV-3150) and photoluminescence spectrofluorometer (FluoroMax-4) with a deuterium lamp radiation source, respectively. All measurements were conducted at room temperature.

3. Results and discussion

3.1. Microstructure of nitrogen-doped ZnO film

Figure 1 presents the X-ray diffraction patterns of the nitrogen-doped ZnO films using different HMT concentrations. The films with and without hydrothermal reactions possess hexagonal wurtzite structures and are *c*-axis (002) oriented with a (101) diffraction peak, in good agreement with previous reports.[2,17–19] The hydrothermal reaction produces a clear shift of the ZnO (002) diffraction peaks closely related to the lattice strain, indicating that the N ions successfully diffuse into the ZnO crystal lattice. The hydrothermal reaction only produces $(NH)_2^-$ to substitute for oxygen by nitrogen breaking down zinc–oxygen bonds and forming zinc–nitrogen bonds. The detailed effect of the HMT concentration on the crystalline structure is determined by carefully analyzing the X-ray diffraction spectra.

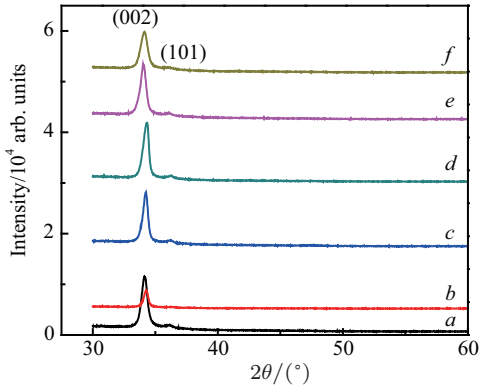


Fig. 1. (color online) X-ray diffraction patterns of the nitrogen-doped ZnO films using HMT concentrations of curve *a* 0.000 M, curve *b* 0.005 M, curve *c* 0.010 M, curve *d* 0.015 M, curve *e* 0.020 M and curve *f* 0.025 M, respectively.

The broadening of the X-ray diffraction peak caused by the grain size and lattice strain can be calculated by the following formula:

$$B^2 = B_{\mathrm{M}}^2 - B_{\mathrm{S}}^2, \tag{4}$$

where B_{M} and B_{S} are the measured full-width at half-maximum (FWHM) and standard FWHM of the guide samples, respectively. The relationship between the average grain size, lattice strain, and FWHM can be described as follows:[14]

$$B\cos\theta = \lambda/\mathrm{size} + 4 \times \mathrm{strain} \times \sin\theta, \tag{5}$$

where λ, θ, size, and strain are the X-ray wavelength, diffraction angle, average grain size, and lattice strain, respectively. Table 1 presents the values of calculated average grain size and lattice strain along the $\langle 002 \rangle$ orientation in terms of Eqs. (4) and (5). The detailed data process can be referred to Ref.[20]. With the increase of HMT concentration, the average grain size along the $\langle 002 \rangle$ direction almost immediately decreases and then increases monotonically. Conversely, the lattice strain first increases and then decreases. At 0.015 M HMT, the average grain size is smallest and the lattice strain is largest. The change in average grain size and lattice strain can be attributed to the enhanced nitrogen doping with HMT increasing. The nitrogen doping first reduces the grain size and enhances the lattice strain, and then increases the grain size and reduces the lattice strain as determined by the number of nitrogen dopants in the ZnO lattice.

Table 1. Calculated values of average grain size and lattice strain along the $\langle 002 \rangle$ orientation.

HMT Conc./M	FWHM/(°)	2θ/(°)	Grain size/nm	Lattice strain/%
0.005	0.184	34.388	99.0	0.218
0.01	0.268	34.222	49.5	0.352
0.015	0.268	34.369	49.5	0.351
0.02	0.234	34.351	62.1	0.299
0.025	0.201	34.168	82.3	0.248
0.03	0.184	34.188	98.9	0.219

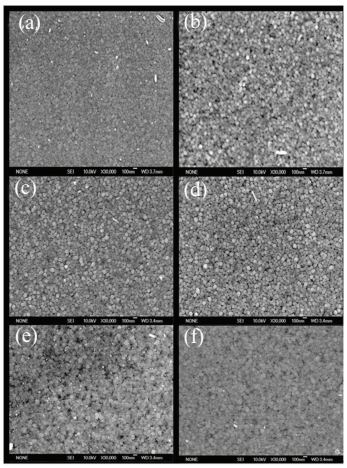


Fig. 2. Surface morphologies of the nitrogen-doped ZnO films using HMT concentrations of (a) 0.000 M, (b) 0.005 M, (c) 0.010 M, (d) 0.015 M, (e) 0.020 M, (f) 0.025 M, respectively.

Figure 2 shows the surface morphologies of the ZnO films using different HMT concentrations. The undoped ZnO exhibits homogeneous particle size and well-proportioned particle distribution. However, the surface evolves from a compact and even surface structure to a sparse and rough surface

with HMT concentration increasing. Small holes or hits are obviously formed, indicating that the hydrothermal reaction involves the nitrogen doping and etching processes.

3.2. Optical properties of nitrogen-doped ZnO films

Figures 3(a) and 3(b) show the reflectance and transmittance spectra of the nitrogen-doped ZnO films using different HMT concentrations. Interference oscillations are clearly observed in the reflectance and transmittance spectra. The shifts in the interference oscillations indicate that the thicknesses of the nitrogen-doped ZnO films using different HMT concentrations are slightly reduced. Figure 4 illustrates the average transmissivity of the nitrogen-doped ZnO films with wavelength values ranging from 400 nm to 800 nm using different HTM concentrations. The average transmissivity initially sharply decreases and then increases with HMT concentration increasing. The kick point of the average transmissivity appears at 0.015 M HMT concentration. The transmissivity and average grain size have similar change tendencies, indicating that the transmissivity is inherently related closely to the grain size-related grain scattering.

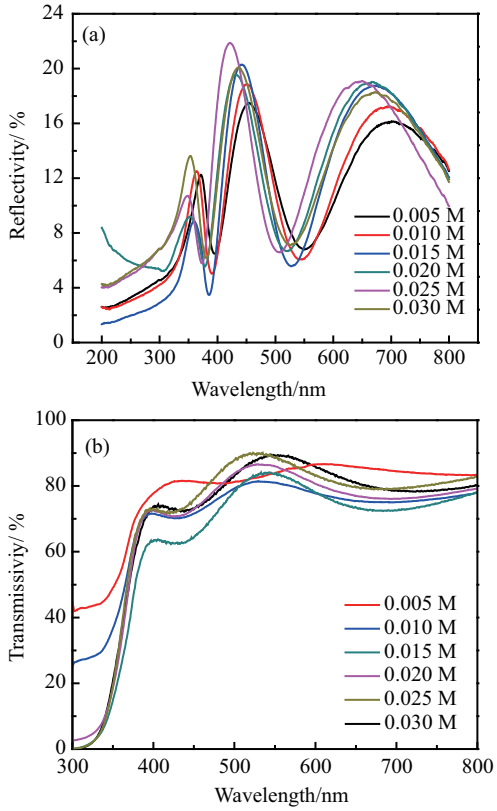


Fig. 3. (color online) (a) Reflectance and (b) transmittance spectra of the nitrogen-doped ZnO films using different HMT concentrations.

Figure 5 shows the absorption spectra of the nitrogen-doped ZnO films using different HMT concentrations. The inset shows the absorption edge spectrum. The detected absorption edge of the film is first red-shifted and then blue-shifted with the increase of HMT concentration. The measured absorption edge varies from 3.513 eV to 3.196 eV, and reaches a lowest value at 0.015 M HMT concentration. Figure 6 shows the PL spectra of the nitrogen-doped ZnO films using different HMT concentrations. For the undoped ZnO film, the UV emission located at 393 nm is dominant in the PL spectrum, which can be attributed to the near band gap excitonic emission. The visible emission (about 512 nm) related to the oxygen defect[4] in the crystal is indistinguishable. However,

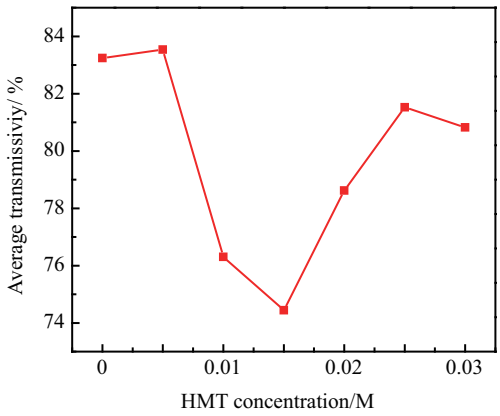


Fig. 4. (color online) Curve of average transmissivity versus HMT concentration of the nitrogen-doped ZnO films with wavelength values ranging from 400 nm to 800 nm.

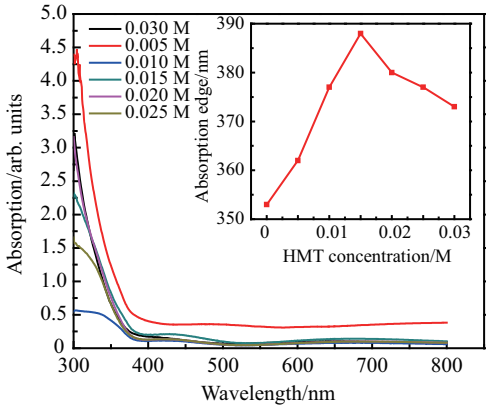


Fig. 5. (color online) Absorption spectra of the nitrogen-doped ZnO films using different HMT concentrations, with the insert showing the absorption edge spectrum.

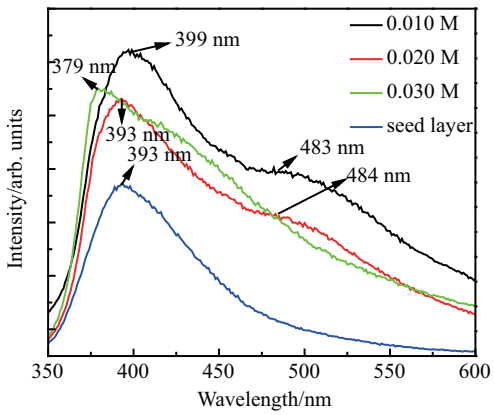


Fig. 6. (color online) Photoluminescence spectra of the nitrogen-doped ZnO films using different HMT concentrations.

for the doped sample, the UV emission basically is first red-shifted (from 393 nm to 399 nm) and then blue-shifted (from 399 nm to 379 nm) with the increase of HMT concentration, which is a trend similar to that of the absorption edge. The visible emission envelope centered near 484 nm is weak compared with the UV emission. The visible emission envelope is mainly related to the nitrogen defect in the crystal. It is noted that the visible emission envelope disappears at an HMT concentration of 0.030 M, revealing that the nitrogen element does not exist in the defect form as the HMT concentration goes beyond 0.030 M. This result is similar to that reported by Li *et al.*[14] and Erdogan *et al.*,[21] who reported on the effect of an N–Li dual-acceptor in ZnO film. Photoluminescence properties of the film are mainly related to the nitrogen-related defects arising from the enhanced nitrogen doping with the increase of HMT concentration.

4. Conclusions

In this paper, nitrogen doping of ZnO films deposited by the magnetron sputtering method is performed by the hydrothermal synthesis method. The effects of HMT concentration on the microstructure and optical properties of the nitrogen-doped ZnO films are investigated. The main conclusions drawn are as follows.

(i) The nitrogen-doped ZnO films preferred a $\langle 002 \rangle$ orientation.

(ii) The hydrothermal reaction of HMT only produced $(NH)_2^-$ to substitute for oxygen by nitrogen breaking down zinc–oxygen bonds and forming zinc–nitrogen bonds. The hydrothermal reaction involves the nitrogen doping and etching processes.

(iii) The structural evolution is attributed to the changes in grain size and lattice strain induced by nitrogen doping. The changes in transmittance property are inherently due to the change in the grain size-related grain scattering with the increase of HMT concentration.

(iv) Photoluminescence properties of the film are mainly related to the nitrogen-related defects arising from the enhanced nitrogen doping with the increase of HMT concentration. For the doped sample, the UV emission is basically first red-shifted (from 393 nm to 399 nm) and then blue-shifted (from 399 nm to 379 nm) with the increase of HMT. The visible emission envelope is mainly attributed to the relation to the nitrogen defect in the crystal.

References

[1] Ding M, Zhao D X, Yao B, Li B H, Zhang Z Z and Shen D Z 2011 *Appl. Phys. Lett.* **98** 062102
[2] Fang X, Li J H, Zhao D X, Shen D Z, Li B H and Wang X H 2009 *J. Phys. Chem.* **113** 21208
[3] Lin S S, Lu J G, Ye Z Z, He H P, Gu X Q, Chen L X, Huang J Y and Zhao B H 2008 *Solid State Commun.* **148** 25
[4] Sun H, Zhang Q, Zhang J, Deng T and Wu J 2008 *Appl. Phys.* B **90** 543
[5] Das S N, Choi J H, Kar J P, Lee T L and Myoung J M 2010 *Mater. Chem. Phys.* **121** 472
[6] Rao R A and Dutta V 2008 *Nanotechnology* **19** 445712
[7] Ramgir N S, Ghosh M, Veerender P, Datta N, Kaur M, Aswal D K and Gupta S K 2011 *Sensor. Actuat.* B **156** 875
[8] Liu N S, Fang G J, Zeng W, Long H, Yuan L Y and Zhao X Z 2011 *J. Phys. Chem.* C **115** 570
[9] Baruah S, Mohammad A M, Myint M T Z, Bora T and Dutta J 2010 *Beilstein J. Nanotechnol.* **1** 14
[10] Ruske F, Sittinger V, Werner W, Szyszka B, van Ostenb K U, Dietrichb K and Rix R 2005 *Surf. Coat. Tech.* **200** 236
[11] Gao X Y, Zhao M K, Zhang Z Y, Chen C, Ma J M and Lu J X 2011 *Thin Solid Films* **519** 6620
[12] Gao X Y, Lin Q G, Feng H L, Liu Y F and Lu J X 2009 *Thin Solid Films* **517** 4684
[13] Lü J G, Huang K, Chen X M, Zhu J B, Meng F M, Song X P and Sun Z Q 2011 *Appl. Surf. Sci.* **257** 2086
[14] Li S S, Zhang Z, Hang J Z, Feng X P and Liu R X 2011 *Chin. Phys.* B **20** 127102
[15] Wang X P, Wang Z, Wang L J and Mei C Y 2011 *Chin. Phys.* B **20** 105203
[16] Guo M, Diao P, Wang X D and Cai S M 2005 *J. Solid State Chem.* **178** 3210
[17] Hook F, Kasemo B, Nylander T, Fant C, Sott K and Elwing H 2001 *Anal. Chem.* **73** 5796
[18] Sieber B, Liu H Q, Piret G, Laureyns J, Roussel P, Gelloz B, Szunerits S and Boukherroub R 2009 *J. Phys. Chem.* **113** 13643
[19] Chen X C, Zhou J P, Wang H Y, Xu P S and Pan G Q 2011 *Chin. Phys.* B **20** 096102
[20] Fan X Y and Ma S M 2002 *China Ceramic Industry* **9** 43 (in Chinese)
[21] Erdogan N H, Kara K, Ozdamar H, Kavak H, Esen R and Karaagac H 2011 *J. Alloys Compd.* **509** 8922